Structural Changes and Crystallization Dynamics of Poly(L-lactide) during the Cold-Crystallization Process Investigated by Infrared and Two-Dimensional Infrared Correlation Spectroscopy

Jianming Zhang,[†] Hideto Tsuji,[‡] Isao Noda,[§] and Yukihiro Ozaki*,[†]

Department of Chemistry, School of Science and Technology, Kwansei-Gakuin University, Gakuen, Sanda 669-1337, Japan; Department of Ecological Engineering, Faculty of Engineering, Toyohashi University of Technology, Tempaku-cho, Toyohashi, Aichi 441-8580, Japan; and The Procter & Gamble Company, 8611 Beckett Road, West Chester, Ohio 45069

Received April 13, 2004; Revised Manuscript Received June 6, 2004

ABSTRACT: The structural evolution and crystallization dynamics of poly(L-lactide) (PLLA) during isothermal cold-crystallization process are studied by infrared (IR) spectroscopy and two-dimensional correlation analysis. In the C═O stretching region, the band shift to a higher wavenumber taking place during the crystallization of PLLA is attributed to the dipole−dipole interaction between the C═O groups. A detailed analysis is performed for the range of 1500−1000 cm^{-1} where bands are highly overlapped. It was found that the 1458 cm^{-1} band reflects the structural order of the CH_3 group, and the band at 1109 cm^{-1} is related to the C−O−C trans conformation in the crystalline phase of PLLA. The band at 1193 cm^{-1} is sensitive not only to the structural adjustment of the C−O−C backbone but also to the structural order of CH_3 group in crystalline phase. From the analysis of the difference spectra and 2D correlation spectra in the 1500−1000 cm^{-1} region, it is shown that the structural adjustment of the CH_3 group unambiguously precedes that of the ester group. Moreover, the detailed crystallization kinetic of PLLA is investigated by analyzing difference spectra.

1. Introduction

In the past decade, great attention has been focused on biodegradable and biocompatible polymers, both from application and ecological perspectives.[1,2] Poly(L-lactide) (PLLA) ($-[CH_2CH(CH_3)COO]_n-$) is a biocompatible semicrystalline polymer, which can be hydrolytically degraded to produce fully biodegradable oligomers. PLLA possesses thermal and mechanical properties useful for many applications and especially superior transparency of the processed materials.[3−6] The mechanical properties and chemical stability of a crystalline polymer, in general, strongly depend on its crystal structures and their morphology. Therefore, the morphology and crystal structure of PLLA have been investigated extensively by AFM, TEM, X-ray scattering, etc.[7−12] Depending on the preparation conditions, three different crystalline modifications (α, β, γ) can be attained for PLLA. Recently, the fine details of dynamic processes during the crystallization of PLLA have become a matter of keen interest. For example, Doi et al.[13,14] successfully observed the initial stage of crystallization and development of lamellae during the isothermal crystallization at 165 °C by using temperature-controlled AFM. Mijoivic et al. also monitored the molecular dynamics of PLLA during the melt and cold crystallization by utilizing broad-band dielectric relaxation spectroscopy (DRS) over a wide range of frequency and temperature.[15]

Fourier transform infrared spectroscopy (FTIR) is sensitive to the conformation and local molecular environment of polymers. Therefore, IR spectroscopy has been used to elucidate the structure of this crystalline polymer.[16] Early IR studies on PLLA mainly focused on the identification of characteristic bands to investigate the polymer crystallinity. In fact, this technique shows many advantages that make it ideal for dynamic studies of the crystalline behavior of polymer. For example, only a small amount of sample is necessary, and precise temperature control can be achieved easily. Moreover, structural evolution at the molecular level can be simultaneously monitored in real time. Therefore, the IR probe has been widely applied to reveal the structural and conformational changes of macromolecules during the melting and crystallization process. There are many examples where the crystallization process of various semicrystalline polymers has been monitored by the FTIR technique.[17−20] However, surprisingly little study has been reported on the structural changes taking place during the melting and crystallization process of PLLA using IR. One of the reasons for this apparent lack of previous IR work may be due to the fact that the spectral region in 1300−1000 cm^{-1} mainly associated with ester groups is highly overlapped, and the detailed analysis and assignment on this spectral region have been difficult. To circumvent this limitation, we use in this study 2D IR correlation spectroscopy in addition to conventional IR methods to elucidate the detailed crystallization dynamics of PLLA.

Since the introduction of generalized two-dimensional (2D) correlation spectroscopy by Noda in 1993,[21−23] this technique has become a powerful and versatile tool for elucidating subtle spectral changes induced by an external perturbation such as temperature, concentration, time, etc. Generalized 2D correlation spectroscopy has gained popularity in the analysis of IR spectra of polymers for two major reasons. One is that 2D spectroscopy enhances apparent spectral resolution by deconvoluting highly overlapped bands into individual

[†] Kwansei-Gakuin University.
[‡] Toyohashi University of Technology.
[§] The Procter & Gamble Company.
* To whom all correspondence should be addressed: Fax +81-79-565-9077; e-mail ozaki@ksc.kwansei.ac.jp.

10.1021/ma049288t CCC: $27.50
Published on Web 07/27/2004

component bands. Another reason is that it gives the information about specific order of the spectral intensity changes taking place during the measurement from the analysis of the asynchronous spectra.

Several important papers have been published concerning the infrared and Raman spectra of PLA. For example, the effects of morphology, conformation, and configuration on the IR and Raman spectra of various poly(lactic acid)s were investigated by Kister et al.[24] A Raman analysis was also conducted to examine the disordered structures of poly(lactic acid).[25] In the present study, the structural changes and crystallization kinetics of PLLA during the cold-crystallization process of PLLA at 78 °C are investigated by using IR spectroscopy. Using conventional spectral analysis methods for IR spectra, such as the difference spectra and second derivatives, together with 2D correlation analysis, the time-dependent IR spectra of PLLA are examined in detail. The isothermal cold crystallization kinetics is analyzed on the basis of difference IR spectra.

2. Experimental Section

2.1. Material and Sample Preparation Procedures. The synthesis and purification of PLLA (PLLA: $M_w \cong 150\,000$ g mol^{-1}, $M_w/M_n = 1.8$) used in the present study were performed according to procedures reported previously.[26] PLLA film for an IR measurement was cast on KBr windows from a 1% (w/v) PLLA chloroform solution. After the majority of the solvent had evaporated, the film was placed under vacuum at room temperature for 48 h to completely remove the residual solvent. Special attention was paid to ensure that the film examined was sufficiently thin to be within the absorption range where the Beer−Lambert law is obeyed. IR spectra verified that the film thus prepared was amorphous.

2.2. FTIR Spectroscopy. For studying the cold crystallization process of PLLA by IR spectroscopy, the sample was set on a homemade variable temperature cell, which was placed in the sample compartment of a Thermo Nicholet Magna 870 spectrometer equipped with a MCT detector. The sample was then heated at 10 °C/min up to 78 °C and annealed for 2 h. All the IR spectra of the specimen were collected at 2 cm^{-1} resolution with 2 min interval during the annealing process at 78 °C. The spectra were obtained by coadding 16 scans.

2.3. 2D IR Correlation Analysis. Before performing the 2D correlation analysis, the IR spectra were preprocessed to minimize the effects of baseline instabilities and other nonselective effects. The wavenumber regions of interest (1840−1680, 1300−1000 cm^{-1}) were truncated first and subjected to a linear baseline correction, followed by offsetting to the zero absorbance value. Ten spectra with an equal temperature interval in a certain wavenumber range were selected for the 2D correlation analysis, which was carried out by using the software named "2D Pocha" composed by D. Adachi (Kwansei Gakuin University). The temperature-averaged 1D reference spectrum is shown at the side and top of the 2D correlation map for reference. In the 2D correlation map, areas without dots indicate positive correlation intensities, while those with dots indicate negative correlation intensities.

3. Results and Discussion

3.1. Structure Formation and Bands Assignment. To elucidate structural changes during the cold-crystallization process of PLLA, we first investigate the spectral difference between amorphous and semicrystalline PLLA samples. Figure 1 shows IR spectra of the PLLA cast film used for cold crystallization before and after annealing at 78 °C for 2 h. The enlarged spectra region in the 1000−800 cm^{-1} is plotted in the inset graph of Figure 1. The IR spectrum of the PLLA cast film before annealing shows the complete lack of the

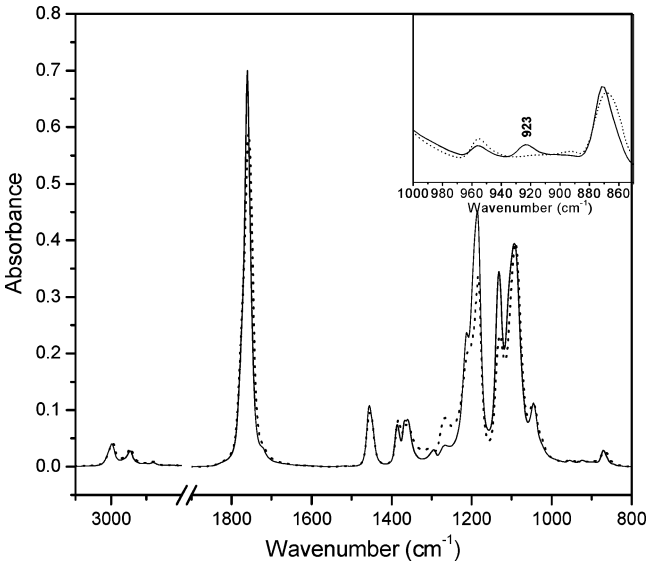

Figure 1. IR spectra of the PLLA samples used for cold crystallization before (···) and after (—) annealing at 78 °C for 2 h.

band at 923 cm^{-1}, which is assigned to the coupling of C−C backbone stretching with the CH_3 rocking mode and sensitive to the 10_3 helix chain conformation of PLLA α crystals.[27−29] It indicates that the sample prepared for the cold crystallization is initially in the amorphous state, and α crystals of PLLA were formed after the cold crystallization at 78 °C for 2 h.

It should be pointed out that the crystalline structure of the α form of PLLA has yet to be assigned definitively. For example, Hoogsten et al.[9] observed extra 00*l* reflections which suggest some deviation from a "pure" 10_3 helix conformation. Recent research by potential energy calculations has also shown that a distorted helix exists in α crystals of PLLA.[30] However, there is no doubt that the 923 cm^{-1} band is related to the α crystals of PLLA. Obviously, the IR spectra of amorphous and semicrystalline PLLA yield distinct differences (Figure 1). It is noted that two regions of the IR spectra are very sensitive to the structural changes taking place during the crystallization process of PLLA. One is the C═O stretching vibration region of 1860−1660 cm^{-1}, and the other is the region of 1500−1000 cm^{-1} which is involved in the CH_3, CH bending, and C−O−C stretching vibration. In contrast, the spectral change of the C−H stretching vibration in the high wavenumber region of 3000−2800 cm^{-1} is relatively very small. Detailed analysis and discussion on the two crystallization-sensitive regions will be shown separately as below.

3.1.1. C═O Stretching Region. The spectral evolution in the C═O stretching region during the cold-crystallization process is shown in Figure 2a. Difference spectra calculated by subtracting the initial spectrum from the rest of spectra in Figure 2a are displayed in Figure 2b. Obviously, during the crystallization process, the intensity of a positive peak at 1762 cm^{-1} increases gradually with time, while that of a negative peak at 1749 cm^{-1} decreases. It seems rational to assign the 1762 cm^{-1} band to the ν(C═O) in the crystalline phase and the 1749 cm^{-1} band to the ν(C═O) in the amorphous phase. However, from the second derivative (Figure 3) of the spectra shown in Figure 2a, no two fixed peak position can be observed in the ν(C═O) spectral region, and only a high-wavenumber shift is observed. Therefore, the positive and negative differential absorbance

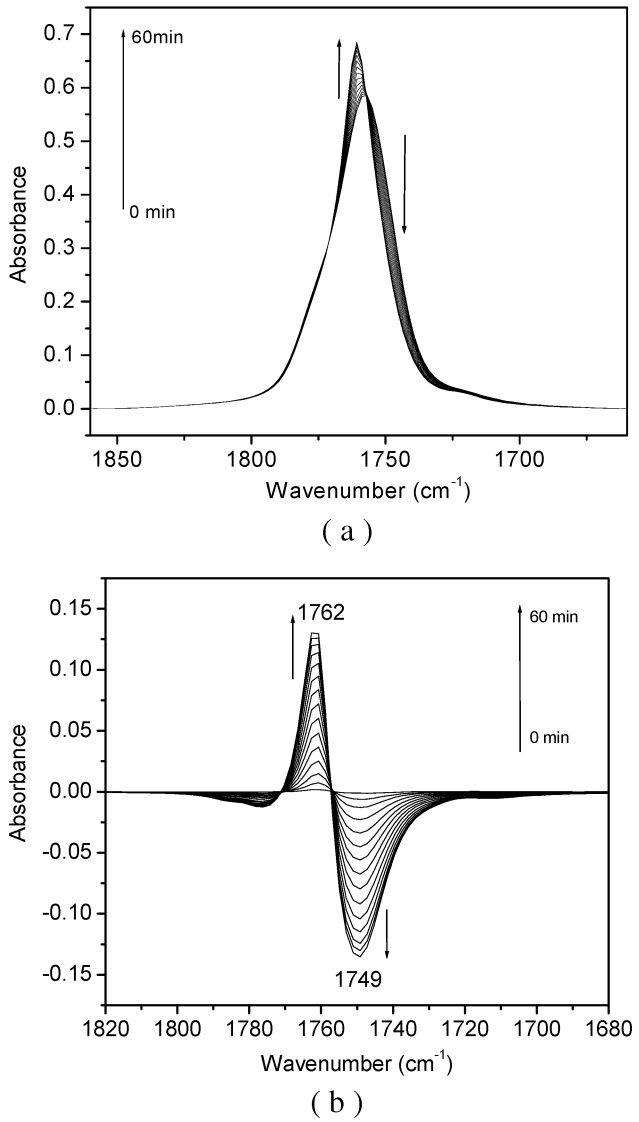

Figure 2. (a) Temporal changes of the IR spectrum in the wavenumber range of 1860−1660 cm^{-1} during the cold-crystallization process of PLLA at 78 °C. The spectra were arranged with a 4 min interval. (b) Difference spectra obtained by subtraction of the initial spectrum from the spectra shown in (a).

peaks in the difference spectra in the 1840−1680 cm^{-1} region maybe artificially generated in the difference spectra by the crystallization-induced frequency shift and bandwidth narrowing of the actual IR spectra. In general, the asynchronous 2D correlation spectra have been used to identify the sequential changes of spectral intensities. However, it is found that some features generated in a 2D asynchronous map may be the result of small frequency shifts or bandwidth changes.[31−33] From asynchronous correlation spectra (Figure 4) calculated with the spectra in Figure 2, it is not difficult to see that the so-called "butterfly pattern" appears in the C═O stretching region. Usually, the appearance of such a pattern in an asynchronous spectrum is attributed to a peak shift combined with the intensity changes.[31,32]

On the basis of the analysis above, we can conclude that two-phase model is not suitable for explaining the spectral changes in the ν(C═O) region during the cold-crystallization process of PLLA. Kister et al.[24] reported that the ν(C═O) stretching mode is split into three

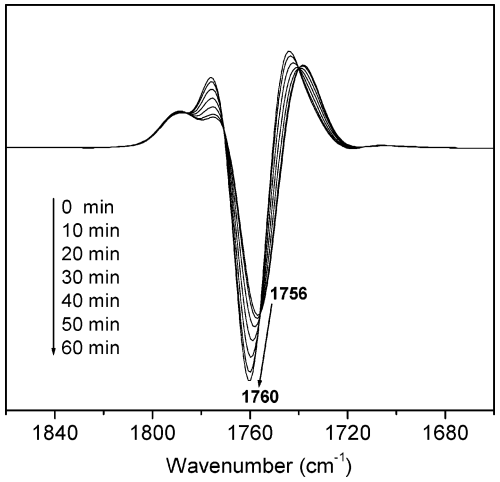

Figure 3. Second derivatives of the spectra shown in Figure 2a.

components in Raman spectra for semicrystalline PLLA. It is well-known that for polymer systems a band splitting occurs due to the dipole−dipole coupling when the molecules form an ordered structure.[34] Usually, the dipole−dipole interaction provides quite different spectral patterns for IR and Raman spectra, which is consistent with the case for semicrystalline PLLA sample. Accordingly, a possible interpretation for the high-frequency shift of the ν(C═O) band is due to the transition dipole coupling of the C═O bonds in the crystalline state. Moreover, according to the crystal structure of PLLA revealed by X-ray crystallography,[9] the PLLA chains form a distorted 10_3 helical structure in α crystals, and its crystal unit cell contains two left-handed helical molecules in antiparallel orientation. However, the distance between the neighboring C═O groups along the chain can be estimated to be 3.26 Å from the crystal structure revealed by X-ray crystallography, which is larger than the distance (∼2.7 Å) for inducing the dipole−dipole interaction.[35] Therefore, one may speculate that the dipole−dipole interaction between the C═O groups belongs to the interchain interaction and not intrachain interaction during the crystallization process of PLLA.

3.1.2. CH_3 and CH Bending and C−O−C Stretching Region. In this study, we are particularly interested in the range from 1500 to 1000 cm^{-1}, which is highly sensitive to the crystallization process, but detailed analysis in this spectral region has been somewhat lacking. Figure 5a shows the spectral changes of the PLLA cast film in the region of 1500−1000 cm^{-1} as a function of annealing time. As the crystallization progresses at 78 °C, the intensities of some bands change greatly, and the others show a frequency shift. From the original spectral data shown in Figure 5a, the bands in the 1500−1300 cm^{-1} region, which are assigned to the deformation vibrations of the CH_3 group and the bending vibration of CH group, show only slight changes. A band around 1454 cm^{-1} is assigned to the CH_3 asymmetric deformation mode, which can usually be taken as an internal standard.[24] It is noted that this band shows a small high-wavenumber shift and intensity increase during the crystallization. This phenomenon has not been noted in the literature. The high-wavenumber shift of this band is probably caused by the appearance of a new peak at a high wavenumber that corresponds to the development of the crystalline phase. Usually, the convolution of the old and new peaks

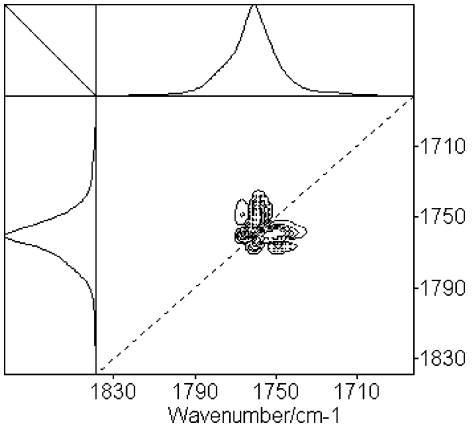

Figure 4. Asynchronous correlation spectra of PLLA in the region of 1840−1680 cm^{-1} calculated from the spectra obtained during annealing at 78 °C.

produces the apparent shift. Subsequently, the difference spectra verify that the new band relating to the crystallization process does appear in this spectral region. A band around 1384 cm^{-1} is due to the CH_3 symmetric deformation mode, and bands in 1368−1360 cm^{-1} may be associated with the combination of $\delta_s(CH_3)$ and $\delta(CH)$. Some small spectral changes take place for these bands, while relatively large changes occur in the C−O−C stretching region from 1300 to 1000 cm^{-1}. To emphasize the spectral changes and to relate the intensity changes of these peaks to the crystallization kinetics, a series of difference spectra are calculated by subtracting the initial (amorphous state) spectrum from the semicrystalline state spectra displayed in Figure 5a. Figure 5b depicts them. The difference spectra show two interesting new features: one is a symmetric positive peak appearing at 1458 cm^{-1}, and the other is a pair of double positive peaks occurring in the 1368−1359 cm^{-1} region. These new peaks all show positive intensities in the difference spectra. The new features at 1458, 1368, and 1359 cm^{-1} should be related to the structural order of the CH_3 group in the crystalline phase during the cold crystallization of PLLA at 78 °C.

In the 1300−1000 cm^{-1} region, pronounced spectral changes during the cold crystallization could be observed not only in the original spectra in Figure 5a but also in the difference spectra in Figure 5b. However, bands in this region are heavily overlapped, and thus the second-derivative IR spectra in the 1000−1300 cm^{-1} region are calculated for the amorphous and semicrystalline PLLA films measured at before and after annealing at 78 °C (Figure 6). It should be noted that there are some small differences in the peak positions between the second-derivative spectra and the difference spectra. Six component bands are revealed in this region for the amorphous PLLA sample, whereas eight bands for the semicrystalline sample. Two bands around 1194 and 1107 cm^{-1}, which do not appear in the spectrum of the amorphous PLLA sample, may be characteristic of the crystalline state. According to the literature,[24,26] the bands at 1183 and 1212 cm^{-1} of the amorphous PLLA are assigned to the combination of $\nu_{as}(C-O-C)$ and $r_{as}(CH_3)$.

In the crystalline state, the band at 1212 cm^{-1} shifts to 1215 cm^{-1}, whereas the band at 1183 cm^{-1} splits into two bands at 1194 and 1184 cm^{-1}. A similar case can also be seen in the $\nu_s(C-O-C)$ region, where only one band appears at 1089 cm^{-1} for the amorphous state, but two bands are observed at 1107 and 1089 cm^{-1} for the

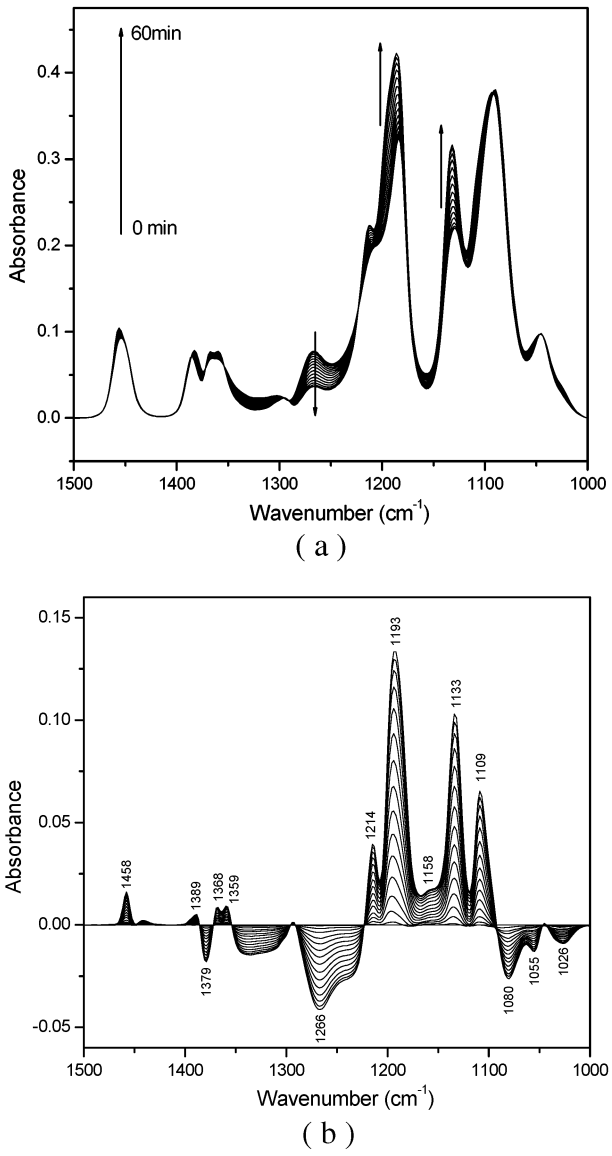

Figure 5. (a) Temporal changes of the IR spectrum in the wavenumber range of 1500−1000 cm^{-1} during the cold crystallization process of PLLA at 78 °C. The spectra were collected with 4 min interval. (b) Difference spectra obtained by subtraction of the initial spectrum from the spectra shown in (a).

crystalline state. During the crystallization of PLLA, the adjustment of the conformation of C−O−C backbone seems to be a precondition for the formation of the ordered helix conformation of polymer chain. Moreover, in the difference spectra shown in Figure 5b, the band intensities around 1194 and 1107 cm^{-1} increase with the annealing time. Therefore, it is rational to propose that the two new bands due to the vibrational modes involving the C−O−C stretching vibrations are related with the planar trans conformational state of ester group in the crystalline phase of PLLA. The other two bands (1133 and 1044 cm^{-1}) appearing in both the amorphous and crystalline states are assigned respectively to the CH_3 rocking and C−CH_3 stretching mode. Table 1 lists band assignments of the amorphous and semicrystalline PLLA samples in the range 1500−1000 cm^{-1}.

3.2. Crystallization Kinetics. To investigate the crystallization kinetics, normalized peak heights of the crystalline sensitive bands at 1458, 1193, 1133, and

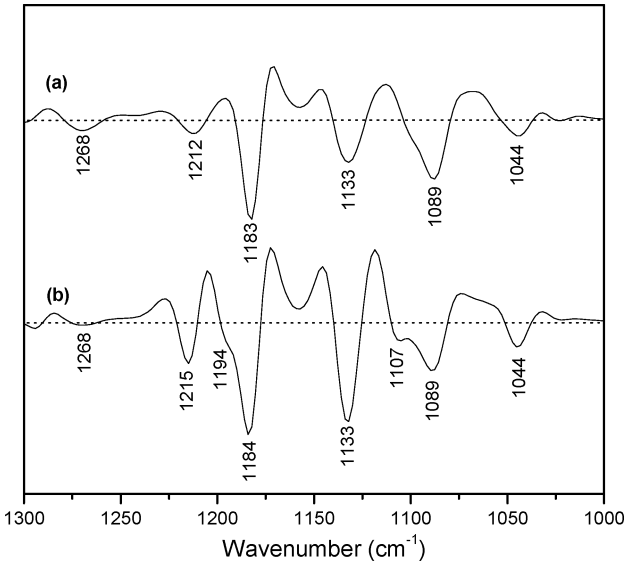

Figure 6. Second-derivative IR spectra in the region of 1300−1000 cm^{-1} for the PLLA sample (a) in the amorphous and (b) semicrystalline state PLLA at 78 °C.

Table 1. Band Assignments of Amorphous and Semicrystalline PLLA in the 500−1000 cm^{-1} Region

IR frequencies (cm^{-1})		
amorphous	semicrystalline	assignments
1454	1458	$\delta_{as}(CH_3)$
1383	1386	$\delta_s(CH_3)$
1363	1368	δ(CH), CH wagging (bending)
	1360	
1268	1268	ν(CH) + ν(COC)
1212	1215	ν_{as}(COC) + $r_{as}(CH_3)$
1182	1194	
	1184	
1133	1133	$r_s(CH_3)$
1089	1107	ν_s(COC)
	1089	
1044	1044	ν(C−CH_3)

1109 cm^{-1} of PLLA are plotted as a function of crystallization time at 78 °C in Figure 7. An interesting result is that the 1193 cm^{-1} band shows the fastest rate of change while the 1109 cm^{-1} band shows the slowest. The order of intensity changes is as follows: 1193 cm^{-1} > 1458 ≈ 1133 cm^{-1} > 1109 cm^{-1}. According to the band assignments above, the 1193 cm^{-1} band is assigned to ν_{as}(C−O−C) + $r_{as}(CH_3)$, and the bands at 1458 and 1133 cm^{-1} are the pure band relative to the CH_3 group. The 1109 cm^{-1} band is due to ν_s(C−O−C), which is a pure band relative to the C−O−C backbone of PLLA. In the previous analysis, we have pointed out that the bands located around 1193 and 1109 cm^{-1} are both sensitive to the C−O−C trans conformation in the crystalline phase of PLLA, whereas the band at 1458 cm^{-1} reflects the structure order of the CH_3 group in the crystalline phase. However, from the sequence of intensity changes shown in Figure 7, additional conclusions may be drawn. Considering the band assignments and the order of intensity changes, the proper description may be given as follows: the band at 1193 cm^{-1} is sensitive not only to the structural adjustment of the C−O−C backbone but also to the structural order of the CH_3 group. Under such consideration, we can derive a molecular level mechanism that the structural adjustment of CH_3 group occurs faster than that of C−O−C group during the crystalline process of bulk PLLA. From the molecular structure of PLLA repeat unit, this conclusion also seems to be reasonable. At the same time, the reason for the fastest changing rate of the 1193 cm^{-1} band can also be provided.

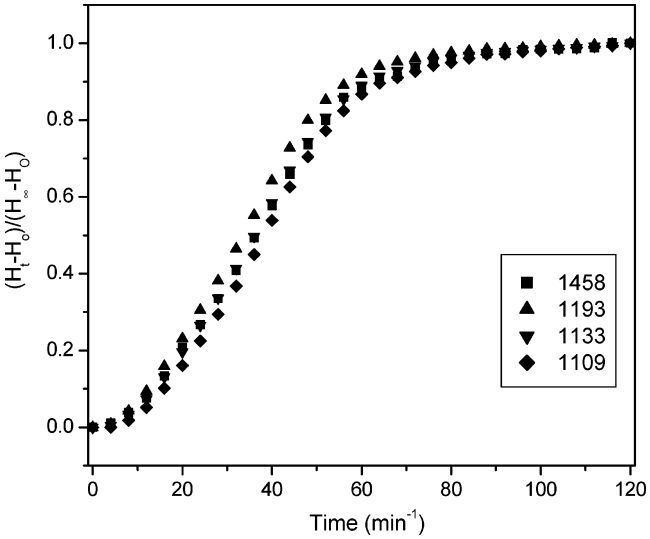

Figure 7. Normalized peak heights of the crystalline sensitive bands at 1458, 1193, 1133, and 1109 cm^{-1} of PLLA as a function of crystallization time at 78 °C calculated from the difference spectra shown in Figure 5b.

It has been well established that the information about the specific order of spectral intensity changes taking place during the measurement can also be derived from the analysis of the 2D asynchronous spectra. To confirm the conclusion above, we further investigate the 2D correlation spectra of PLLA calculated from the spectra obtained during annealing at 78 °C. Figure 8a,b shows the synchronous $\Phi(\nu_1,\nu_2)$ and asynchronous $\Psi(\nu_1,\nu_2)$ 2D correlation spectra. In both 2D spectra, it can be seen that highly overlapped peaks in the range 1300−1000 cm^{-1} are deconvoluted effectively by spreading the peaks along the second spectral dimension. An asynchronous spectrum represents sequential or successive changes of spectral intensities measured at ν_1 and ν_2. According to Noda's rule,[21,22] the sign of an asynchronous cross-peak becomes positive if the intensity change at ν_1 occurs predominantly before ν_2 in the sequential order of t. It becomes negative, on the other hand, if the change occurs after ν_2. This rule is, however, reversed if the corresponding synchronous intensity becomes negative, i.e., $\Phi(\nu_1,\nu_2) < 0$. Compared with the synchronous spectrum in Figure 8a, the corresponding asynchronous spectrum in Figure 8b is more strongly influenced by fine details of spectral fluctuations. The information about the sequential changes of the bands at 1193, 1133, and 1109 cm^{-1} can be obtained from several well-separated cross-peaks in Figure 8a,b. In the synchronous spectrum (Figure 8a), Φ(1193, 1133), Φ(1193, 1109), and Φ(1133, 1109) > 0, and in the corresponding asynchronous spectrum Ψ (1193, 1133), Ψ (1193, 1109), and Ψ (1133, 1109) > 0 (Figure 8b). These observations indicate that the sequential order of these three bands is 1193 cm^{-1} > 1133 cm^{-1} > 1109 cm^{-1}, which is consistent with the result of Figure 7. Therefore, from the 2D correlation analysis, the same sequential order can also be derived.

Usually, it is believed that the structural changes of various functionalities within a polymer occur cooperatively during the crystallization. However, in the case of cold crystallization of PLLA, different rates of changes

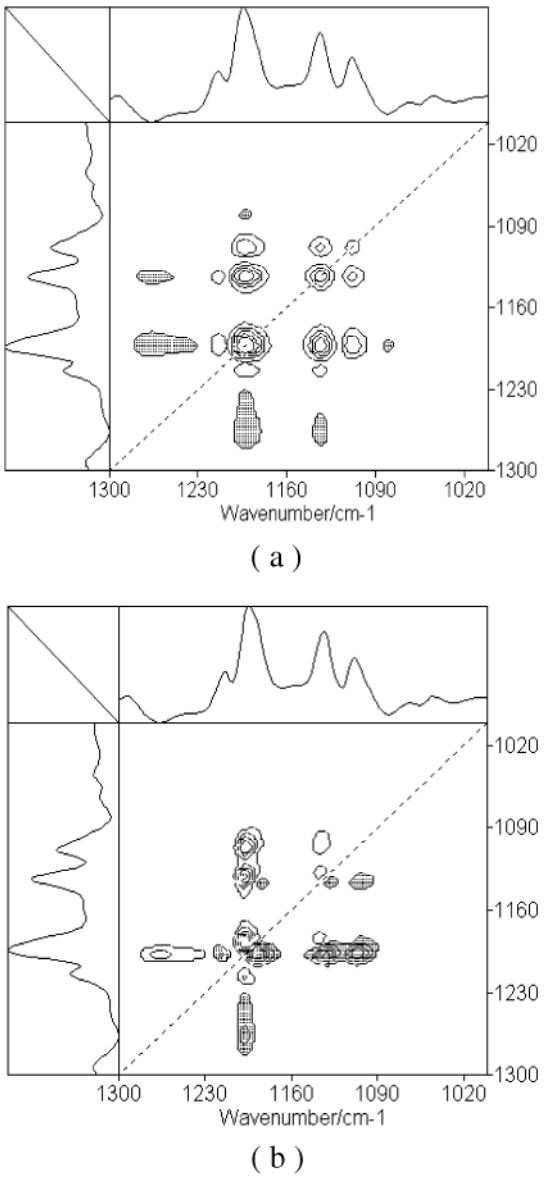

Figure 8. Synchronous (a) and asynchronous (b) correlation spectra of PLLA in the region of 1300−1000 cm^{-1} calculated from the spectra obtained during the annealing at 78 °C.

for the CH_3 and ester groups are unambiguously verified by the analysis of 1D and 2D spectra. To explain the distorted helix conformation in α crystals of PLLA, Hoogsteen et al.[9] suggested that the interchain contacts between CH_3 groups force this distortion, in a way similar to the α-helix conformation of poly(L-alanine), which is the polypeptide analogue of poly(L-lactide). Therefore, it seems that the difference in the rate of changes between CH_3 group and C−O−C group during the process of α crystals formation of PLLA should be related to the interchain interaction between the CH_3 groups.

The well-known Avrami equation[36,37] is often used to analyze the isothermal crystallization process of polymer. When IR data in difference spectra are used, Avrami's equation can be stated as follows:

$$\frac{A_t - A_\infty}{A_0 - A_\infty} = \exp(-kt^n) \qquad (1)$$

where A_t is the peak intensity at the crystallization time

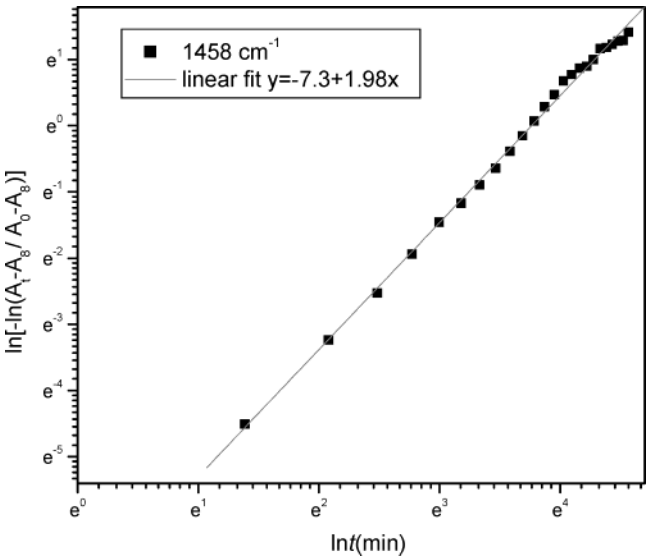

Figure 9. An example of the plot of Avrami equation for the isothermal cold crystallization of PLLA at 78 °C. The peak height of the band at 1458 cm^{-1} is used for this plot.

Table 2. Avrami Parameters Derived from the Analysis of Isothermal Cold Crystallization of PLLA by Using the Normalized Peak Heights As Shown in Figure 7

	bands used for calculation (cm^{-1})				
parameters	1458	1193	1133	1109	av
rate constant, k ($min^{-n} \times 10^4$)	6.75	6.75	3.85	2.75	7.34
Avrami index, n	1.98	1.98	2.08	2.14	2.02
half-time, $t_{1/2}$ (min)	33	33	37	39	36

t, A_∞ and A_0 are respectively the initial and final peak intensities during isothermal crystallization, k is the crystallization rate constant dependent on the nucleation and growth rates, t is the time of the crystallization, and n is the Avrami exponent, which is related to the nature of nucleation and to the geometry of the growing crystals.[38] Equation 1 can also be expressed in the following form.

$$\ln\left[-\ln\left(\frac{A_t - A_\infty}{A_0 - A_\infty}\right)\right] = \ln k + n \ln t \qquad (2)$$

Accordingly, the Avrami parameters n and k can be obtained from the slope and the intercept, respectively, by plotting the first term versus ln t. Figure 9 gives an example of the plot of Avrami equation using the peak height of the band at 1458 cm^{-1} for the isothermal cold crystallization of PLLA at 78 °C. The curve shows an initial linear portion that subsequently tends to level off. This deviation maybe thought to be due to the secondary crystallization that is caused by the spherulite impingement in the later stage.

The half-life, $t_{1/2}$, is an important parameter for the discussion of the crystallization kinetics and can be expressed as follows:

$$t_{1/2} = \left(\frac{\ln 2}{k}\right)^{1/n} \qquad (3)$$

The parameters of crystallization kinetics calculated according to different bands shown in Figure 7 are listed in Table 2. It can be seen that the variations in these crystalline parameters calculated from different bands

are very small. For isothermal cold crystallization of PLLA at 78 °C, the average value of the Avrami exponent is $n \approx 2$, which suggests that the crystallization started from heterogeneous nucleation and the primary crystallization stage might correspond to a two-dimensional, circular, diffusion-controlled growth of nucleation.

3.3. Conclusion. The IR spectral variations and band assignments during the cold crystallization of PLLA at 78 °C have been investigated in detail by conventional spectral analysis methods as well as 2D correlation analysis. In the C═O region, a high wavenumber shift has been attributed to the dipole−dipole interaction between the C═O groups taking place during the crystallization of PLLA. Several new bands reflecting the structural order of polymer chain have been disclosed in the range 1500−1000 cm^{-1}. Among these crystalline sensitive bands, the 1458 cm^{-1} band has been assigned to the structural order of the CH_3 group, and the band at 1109 cm^{-1} relates to the C−O−C trans conformation in the crystalline phase of PLLA. The band at 1193 cm^{-1} is sensitive not only to the structural adjustment of C−O−C but also to the structural order of CH_3 group in the crystalline phase. It has been shown that the structural adjustment of the CH_3 groups precedes that of ester backbone form the analysis of the 1D spectra and the 2D correlation spectra. Moreover, the isothermal cold-crystallization kinetics of PLLA has been investigated by the data of difference spectra. The Avrami equation describes the primary stage of isothermal crystallization kinetics with the exponent $n \approx 2$ for the cold crystallization of PLLA at 78 °C.

Acknowledgment. Jianming Zhang thanks the Japan Society for the Promotion of Science (JSPS) for financial support.

References and Notes

(1) Khon, J.; Langer, R. In *Biomaterial Science*; Ratner et al., Eds.; Academic Press: New York, 1996.
(2) Ikada, Y.; Tsuji, H. *Macromol. Rapid Commun.* **2000**, *21*, 117.
(3) Tsuji, H.; Ikada, Y. *J. Appl. Polym. Sci.* **1998**, *67*, 405.
(4) Tsuji, H.; Ikada, Y. *Macromol. Chem. Phys.* **1996**, *197*, 3483.
(5) Urayama, H.; Kanamori, T.; Kimura, Y. *Macromol. Mater. Eng.* **2002**, *287*, 116−121.
(6) Dorgan, J. R. *Poly(lactic acid) Properties and Prospects of an Environmentally Benign Plastic*; American Chemical Society: Washington, DC, 1999; pp 145−149.
(7) Eling, B.; Gogolewski, S.; Pennings, A. J. *Polymer* **1982**, *23*, 1587.
(8) Kobayashi, J.; Asahi, T.; Ichiki, M.; Okikawa, A.; Suzuki, H.; Watanabe, T.; Fukada, E.; Shikinami, Y. *J. Appl. Phys.* **1995**, *77*, 2957.
(9) Hoogsteen, W.; Postema, A. R.; Pennings, A. J.; ten Brinke, G. *Macromolecules* **1990**, *23*, 634.
(10) Cartier, L.; Okihara, T.; Ikada, Y.; Tsuji, H.; Puiggali, J.; Lotz, B. *Polymer* **2000**, *41*, 8909.
(11) Puiggali, J.; Ikada, Y.; Tsuji, H.; Cartier, L.; Okinara, T.; Lotz, B. *Polymer* **2000**, *41*, 8921.
(12) Brizzolara, D.; Cantow, H.-J.; Diederichs, K.; Keller, E.; Domv, A. J. *Macromolecules* **1996**, *29*, 191.
(13) Kikkawa, Y.; Abe, H.; Iwata, T.; Inoue, Y.; Doi, Y. *Biomacromolecules* **2001**, *2*, 940.
(14) Abe, H.; Kikkawa, Y.; Inoue, Y.; Doi, Y. *Biomacromolecules* **2001**, *2*, 1007.
(15) Mijovic, J.; Sy, J. W. *Macromolecules* **2002**, *35*, 6370.
(16) Chalmers, J. M.; Hannah, R. W.; Mayo, D. W. Spectra-structure correlations: Polymer spectra. In *Handbook of Vibrational Spectroscopy*; Chalmers, J. M., Griffiths, P. R., Eds.; John Wiley & Sons, Ltd: London, UK, 2002; Vol. 4, pp 1893−1918.
(17) Tashiro, K.; Sasaki, S.; Kobayashi, M. *Macromolecules* **1996**, *29*, 7460.
(18) Duan, Y. X.; Zhang, J. M.; Shen, D. Y.; Yan, S. K. *Macromolecules* **2003**, *36*, 4847.
(19) Healey, A. M.; Hendra, P. J.; West, Y. D. *Polymer* **1996**, *37*, 4009.
(20) Heintz, A. M.; McKiernan, R. L.; Gido, S. P.; Penelle, J.; Hsu, S. L.; Sasaki, S.; Takahara, A.; Kajiyama, T. *Macromolecules* **2002**, *35*, 3117.
(21) Noda, I. *Appl. Spectrosc.* **1993**, *47*, 1329.
(22) Noda, I. *Appl. Spectrosc.* **2000**, *54*, 994.
(23) Noda, I.; Dowrey, A. E.; Marcott, C.; Story, G. M.; Ozaki, Y. *Appl. Spectrosc.* **2000**, *54*, 236A.
(24) Kister, G.; Cassanas, G.; Vert, M. *Polymer***1998**, *39*, 267.
(25) Kang, S.; Hsu, S. L.; Stidham, H. D.; Smith, P. B.; Leugers, M. A.; Yang, X. *Macromolecules* **2001**, *34*, 4542.
(26) Tsuji, H.; Ikada, Y. *Polymer* **1999**, *40*, 6699.
(27) Cohn, D.; Younes, H. *J. Biomed. Mater. Res.* **1988**, *22*, 993.
(28) Lee, J. K.; Lee, K. H.; Jin, B. S. *Eur. Polym. J.* **2001**, *37*, 907.
(29) Sawai, D.; Takahashi, K.; Sasashige, A.; Kanamoto, T. *Macromolecules* **2003**, *36*, 3601.
(30) Sasaki, S.; Asakura, T. *Macromolecules* **2003**, *36*, 8385.
(31) Czarnecki, M. A. *Appl. Spectrosc.* **2000**, *52*, 1583.
(32) Czarnecki, M. A. *Appl. Spectrosc.* **2000**, *54*, 986.
(33) Huang, H.; Malkov, S.; Coleman, M.; Painter, P. *Macromolecules* **2003**, *36*, 8148.
(34) Mallapragada, S. K.; Narasimhan, B. Infrared Spectroscopy in Analysis of Polymer Crystallinity. In *Encyclopedia of Analytical Chemistry*; Meyers, R. A., Eds.; John Wiley & Sons, Ltd: London, UK, 2000; pp 7644−7658.
(35) Lagaron, J. M. *Macromol. Symp.* **2002**, *184*, 19.
(36) Avrami, M. *J. Chem. Phys.* **1939**, *7*, 1103.
(37) Avrami, M. *J. Chem. Phys.* **1940**, *8*, 212.
(38) Qin, Z. B.; Mo Z. S.; Zhang, H. F.; Sheng, S. R.; Song, C. S. *J. Polym. Sci., Part B: Polym. Phys.* **1993**, *31*, 371.

MA049288T